

## Model for Production of $\pi^+$ and $\pi^-$ by Protons from Nuclei

Morton M. Sternheim\* and Richard R. Silbar†

*Los Alamos Scientific Laboratory, University of California, Los Alamos, New Mexico 87544*

(Received 4 August 1972)

We have modified the conventional semiclassical model for pion production from nuclei by including charge exchange of the outgoing pions and by dropping the forward-production approximation. We find good agreement with the general features of the  $\pi^+$  and  $\pi^-$  production by 740-MeV protons from various nuclei, as measured recently by Cochran *et al.*

### I. INTRODUCTION

Cochran *et al.*<sup>1</sup> report extensive measurements of  $\pi^+$  and  $\pi^-$  production by 740-MeV protons from 11 nuclei spanning the periodic table. The results include the first substantial  $\pi^-$  production data in this energy region. In addition the measurements extend to larger angles than in earlier experiments. Here we present a simple model which reproduces many of the general features of this data.

Looking at the data, one is impressed by the smooth and relatively slow variations in the curves for  $d\sigma/d\Omega$  and  $d^2\sigma/dT d\Omega$  in going from nucleus to nucleus. This leads us to suspect the possibility of predicting this behavior with a simple quasigeometrical approach.

Earlier calculations of pion production by nuclei,<sup>2-4</sup> as well as ours, are indeed based on a semiclassical picture. Both the incoming protons and outgoing pions are assumed to suffer attenuation due to absorption by the nuclear medium. The production is assumed to occur at some point within the nucleus with a probability determined by the free proton-nucleon production cross section. As has been noted,<sup>2</sup> this picture is mathematically equivalent to using the Glauber formalism<sup>5,6</sup> for incoherent production.

The methods used in the earlier calculations, however, are not adequate for predicting the  $\pi^-$  and/or large-angle production observed in the experiment of Ref. 1. Consequently we introduce two essentially new ingredients for this type of calculation: (1) a more careful treatment of the angular dependence of the pion path length; (2) the effect of charge exchange in augmenting the  $\pi^-$  cross sections. We find qualitative agreement with the observed large-angle production and good agreement with the  $\pi^+/\pi^-$  ratios. Indeed, within the uncertainties due to our approximations, the  $\pi^+/\pi^-$  ratios verify the essential correctness of the isobar production model.<sup>7</sup> At the same time, our geometrical picture provides an explanation for the observed power-law dependences of the  $\pi^+$

and  $\pi^-$  cross sections.

In our calculation we make the approximations of using a uniform-sphere nuclear density and neglecting Fermi motion. Corrections arising from the diffuseness of the nuclear surface<sup>2</sup> and Fermi motion<sup>3</sup> are not negligible. Nonetheless, the present calculation does show the importance of pion charge exchange and the correct treatment of angular dependence. In a future paper we will report a more complete calculation now in progress.

### II. METHOD OF CALCULATION

#### A. The Semiclassical Model

Our basic assumption is that the pion production takes place at some point within the nucleus by the one-step reaction  $NN \rightarrow NN\pi$ , the so-called impulse approximation. The incoming proton flux is attenuated by interactions with the nuclear medium. Similarly, the outgoing pions suffer absorption and charge exchange.

Figure 1 shows the geometry of our model. The incident proton travels in a straight line within the nucleus for a distance  $d_p$ . At the production point  $\vec{r} = (b, z, \phi)$  it makes a pion with kinetic energy  $T$  at an angle  $\theta$  to the incident direction. The pion then emerges from the nucleus after having traveled a straight-line distance  $d_\pi$ . The nucleus is taken to be a uniform sphere of radius  $R$ .

Earlier calculations of this type used the standard Glauber approximation of forward scattering,  $\theta = 0$ ; in this case all  $\phi$  dependence disappears as well. As one might expect, it is important to keep the angular dependence to adequately describe the large-angle cross sections.

Since our nuclear density is constant,

$$\rho = 3/4\pi R^3. \quad (1)$$

The number of protons arriving at  $\vec{r}$  is proportional to

$$P(\vec{r}) = \exp(-A\rho\sigma_p d_p), \quad (2)$$

where

$$d_p = (R^2 - b^2)^{1/2} + z. \quad (3)$$

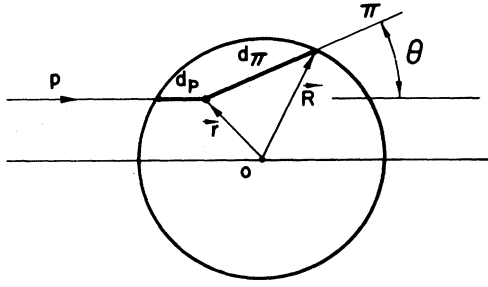


FIG. 1. Model geometry for the case  $\phi = 0$ . In general, the pion is produced at  $\vec{r} = (b, z, \phi)$  and goes out at an angle  $\theta$  to the incident  $z$  direction. The path lengths in the nucleus for the proton and pion are  $d_p$  and  $d_\pi$ , respectively.

The cross section  $\sigma_p$  is the sum of two cross sections,

$$\sigma_p = \sigma_{p, \text{abs}} + \sigma_{p, \text{prod}}. \quad (4)$$

Here  $\sigma_{p, \text{prod}}$  is the cross section for producing a pion of any charge, appropriately averaged over neutrons and protons; an explicit formula will be given in Sec. IIB. Other interactions which leave the proton with insufficient energy to make pions are accounted for by the "absorption cross section"  $\sigma_{p, \text{abs}}$ .

The description of the attenuation of the outgoing pions is complicated by charge exchange. Suppose that  $N_i(0)$  pions of charge states  $i = +, 0, -$  are produced at  $\vec{r}$ . Then, at a distance  $s$  from  $\vec{r}$ , the populations  $N_i(s)$  are determined by

$$\begin{aligned} N_+' &= -\lambda_a N_+ - \lambda_{x, n} N_+ + \lambda_{x, p} N_0, \\ N_0' &= -\lambda_a N_0 - (\lambda_{x, n} + \lambda_{x, p}) N_0 \\ &\quad + \lambda_{x, n} N_+ + \lambda_{x, p} N_-, \\ N_-' &= -\lambda_a N_- - \lambda_{x, p} N_- + \lambda_{x, n} N_0. \end{aligned} \quad (5)$$

Here  $\lambda_a = A\rho\sigma_{\pi, \text{abs}}(T)$  is the inverse mean free path for pion absorption. (Lacking any information on the charge dependence of  $\lambda_a$ , we use a common value for all three equations.) Further,  $\lambda_{x, n} = N\rho\sigma_{\pi, \text{exch}}(T)$  is the inverse mean free path for  $\pi^+ n \rightarrow \pi^0 p$  or  $\pi^0 n \rightarrow \pi^- p$ . Similarly,  $\lambda_{x, p} = Z\rho\sigma_{\pi, \text{exch}}(T)$  corresponds to  $\pi^- p \rightarrow \pi^0 n$  and  $\pi^0 p \rightarrow \pi^+ n$ . We have explicitly noted the energy dependence of pion cross sections.

The solutions for Eq. (5) are obtained by elementary methods and have the form

$$N_i(s) = \sum_j M_{ij}(s, T) N_j(0), \quad (6)$$

where

$$\begin{aligned} M_{ij} = \exp(-\lambda_a s) & [c_{ij}^{(1)} + c_{ij}^{(2)} \exp(-\lambda_S s) \\ & + c_{ij}^{(3)} \exp(-\lambda_L s)], \end{aligned} \quad (7a)$$

$$\lambda_{S, L} = \lambda_{x, n} + \lambda_{x, p} \pm (\lambda_{x, n} \lambda_{x, p})^{1/2}, \quad (7b)$$

$$c_{ij}^{(k)} = c_{ij}^{(k)}(Z/N). \quad (7c)$$

As the coefficients  $c_{ij}^{(k)}$  are rather messy, we refrain from giving them here. We need the  $N_i(s)$  at the surface where

$$s = d_\pi = -l + (l^2 + R^2 - b^2 - z^2)^{1/2}, \quad (8)$$

$$l = b \cos \phi \sin \theta + z \cos \theta.$$

The last factor we need is the probability of producing a pion of charge  $j$  at the interaction point  $\vec{r}$ . This is proportional to the density times the production cross section on free nucleons. Thus, the production cross section for pions of charge  $i$  is

$$\begin{aligned} \frac{d^2 \sigma}{dT d\Omega}(\pi^i) = \sum_j I_{ij} \left( Z \frac{d^2 \sigma(pp \rightarrow NN\pi^j)}{dT d\Omega} \right. \\ \left. + N \frac{d^2 \sigma(pn \rightarrow NN\pi^j)}{dT d\Omega} \right), \end{aligned} \quad (9)$$

$$I_{ij}(T, \theta) = \int d^3 r P(d_p) \rho M_{ij}(d_\pi, T).$$

In the Secs. IIB and IIC we will discuss the various cross sections needed to evaluate the expressions presented in this section.

### B. Isobar-Production Model

One set of inputs required for Eq. (9) is the six free-nucleon pion-production cross sections. Since experimental data<sup>1</sup> are only available for  $pp \rightarrow n p \pi^+$ , we use the isobar model<sup>7</sup> to obtain the other cross sections. In this model we have  $NN \rightarrow N\Delta \rightarrow NN\pi$ , where the  $\Delta$  is the usual (3, 3) resonance at 1231 MeV. Evaluating the appropriate Clebsch-Gordan coefficients and assuming incoherence between different contributions to a given final state gives

$$\begin{aligned} d\sigma(pp \rightarrow \pi^+ n p) &= \frac{5}{8} d\sigma_{\text{iso}}, \\ d\sigma(pp \rightarrow \pi^0 p p) &= \frac{1}{8} d\sigma_{\text{iso}}, \\ d\sigma(pp \rightarrow \pi^- n n) &= 0, \\ d\sigma(pn \rightarrow \pi^+ n n) &= \frac{1}{12} d\sigma_{\text{iso}}, \\ d\sigma(pn \rightarrow \pi^0 n p) &= \frac{1}{3} d\sigma_{\text{iso}}, \\ d\sigma(pn \rightarrow \pi^- p p) &= \frac{1}{12} d\sigma_{\text{iso}}. \end{aligned} \quad (10)$$

Here  $d\sigma_{\text{iso}}$  is the cross section for  $NN \rightarrow N\Delta$  and may be obtained from the measurements of the first of these reactions.

Thus Eq. (9) becomes

$$\frac{d^2 \sigma}{dT d\Omega}(\pi^i) = \frac{6}{5} A \frac{d^2 \sigma(pp \rightarrow n p \pi^+)}{dT d\Omega} \sum_j I_{ij} n_j, \quad (11)$$

where

$$\begin{aligned} n_+ &= (10Z + N)/12A, \\ n_0 &= (Z + 2N)/6A, \\ n_- &= N/12A. \end{aligned} \quad (12)$$

For an  $N=Z$  nucleus,

$$n_+ : n_0 : n_- = 11 : 6 : 1, \quad (13a)$$

while for  $^{208}\text{Pb}$ ,

$$n_+ : n_0 : n_- \approx 7.5 : 5.3 : 1. \quad (13b)$$

Experimentally,<sup>1</sup> the  $\sigma(\pi^+)/\sigma(\pi^-)$  ratio is about 5 for light ( $N \approx Z$ ) nuclei and about 2 for heavy nuclei, considerably less than the ratios in Eqs. (13). The charge-exchange mechanism discussed above must be at least partially responsible for this reduction. Note, however, that the isobar-model predictions given in Eq. (10) involve the assumption of incoherence between various contributions to a given final charge state. Interference effects could conceivably reduce the  $n_+/n_-$  ratio to as little as 5 to 1 in the  $N=Z$  case. The fact that we are able to obtain the observed ratios (see Sec. III) is some evidence for the usual form of the isobar model, as given in Eq. (10).

We also use the isobar-model assumption for the cross section  $\sigma_{\beta, \text{prod}}$  needed in Eq. (4). From Eq. (10),

$$\begin{aligned} \sigma_{\beta, \text{prod}} &= (Z + \frac{1}{2}N)\sigma_{\text{iso}}/A, \\ \sigma_{\text{iso}} &= \frac{6}{5}\sigma(pp \rightarrow np\pi^+) \approx 16 \text{ mb}, \end{aligned} \quad (14)$$

for an incident 740-MeV proton.

The reader might wonder if the isobar production model is consistent with the picture in Sec. II A of production of pions by protons at one point. Since the width of the  $\Delta$  implies a decay length of  $\leq 1$  fm, i.e., less than the mean internucleon distance, there is no substantial inconsistency here.<sup>8</sup>

### C. Other Inputs

In addition to the differential and total  $pp \rightarrow np\pi^+$  cross sections, our model requires three others:  $\sigma_{\beta, \text{abs}}$ ,  $\sigma_{\pi, \text{abs}}$ , and  $\sigma_{\pi, \text{exch}}$ .

The last is the least ambiguous. To the extent that the  $\pi N$  scattering is dominated by the (3, 3) resonance, all the charge-exchange cross sections are equal – this was already assumed in Eq. (5) – and

$$\sigma_{\pi, \text{exch}} = \frac{2}{3}\sigma(\pi^+p). \quad (15)$$

Accurate experimental values of  $\sigma(\pi^+p)$  are available.<sup>9</sup> Note that  $\sigma_{\pi, \text{exch}}$  varies markedly with energy and it would be inappropriate to use a constant value for it.

Very little is known about the proton and pion

absorption cross sections. For the first, we must have

$$\sigma_{\beta, \text{abs}} \leq \frac{Z\sigma_{pp} + N\sigma_{pn}}{A} - \frac{(Z + \frac{1}{2}N)\sigma_{\text{iso}}}{A}, \quad (16)$$

which, at 740 MeV, is  $\approx 33$  mb for all nuclei.<sup>10</sup> A similar bound on  $\sigma_{\pi, \text{abs}}$  does not exist since a large part of pion absorption in nuclei is due to a two-nucleon process. Beder, in his calculation, used a model<sup>11</sup> for  $\sigma_{\pi, \text{abs}}$  which assumed dominance of this ( $\pi, NN$ ) reaction but we obtained rather poor results with his  $\sigma_{\pi, \text{abs}}$ . Perhaps this is because of other important absorptive channels. Regrettably, we could not find any useful experimental information about the cross section for the ( $\pi, X$ ) reaction, where  $X$  contains anything but a pion.

Consequently we adopted an empirical procedure to determine  $\sigma_{\beta, \text{abs}}$  and  $\sigma_{\pi, \text{abs}}$ . We first note that, as either of these increases, the nuclear production cross section will decrease. Or, for a fixed nuclear cross section, increasing  $\sigma_{\beta, \text{abs}}$  requires a compensating decrease in  $\sigma_{\pi, \text{abs}}$ , and vice versa. At the same time we note that the  $\pi^+/\pi^-$  ratio is largely independent of  $\sigma_{\beta, \text{abs}}$  since this only affects the rate at which the pions are produced. But the ratio does depend on  $\sigma_{\pi, \text{abs}}$ ; if  $\sigma_{\pi, \text{abs}}$  is, e.g., small relative to  $\sigma_{\pi, \text{exch}}$ , then there is more time for the initial  $\pi^+$ 's and  $\pi^0$ 's to charge exchange into  $\pi^-$ 's before absorption, hence a smaller  $\pi^+/\pi^-$  ratio. This leads us to expect that  $\sigma_{\beta, \text{abs}}$  and  $\sigma_{\pi, \text{abs}}$  can be chosen to fit both, say, the  $\pi^+$  production cross section and the  $\pi^+/\pi^-$  ratio.

The procedure we actually used is as follows. Presumably the effect of absorption is greatest for heavy nuclei and the error from neglect of multiple scattering is least for small-angle  $\pi^+$  production. Thus, for various choices of  $\sigma_{\beta, \text{abs}}$ , we can evaluate the differential production cross

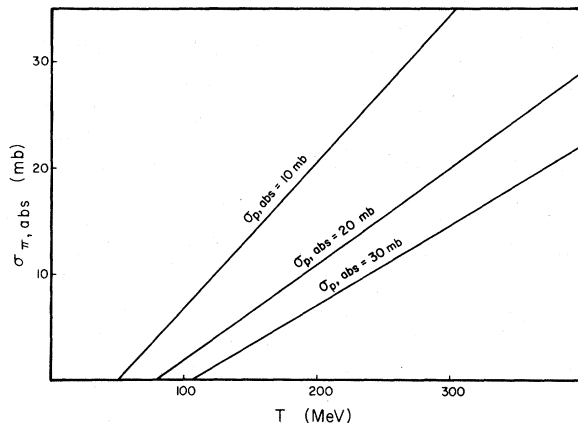


FIG. 2. The pion absorption cross section  $\sigma_{\pi, \text{abs}}(T)$  as fitted to the  $15^\circ \pi^+$  data for Pb, for various values of the proton absorption cross section  $\sigma_{p, \text{abs}}$ .

section with Eq. (11) and adjust  $\sigma_{\pi, \text{abs}}(T)$  to reproduce the measured  $d^2\sigma(\pi^+)/dt d\Omega$  for Pb at  $15^\circ$ .<sup>12</sup> Figure 2 shows eyeball fits for  $\sigma_{\rho, \text{abs}} = 10, 20,$  and  $30$  mb, smoothed into straight lines.

Note that, for each value of  $\sigma_{\rho, \text{abs}}$ , the fitted pion absorption cross sections needed to reproduce the data increase with  $T$ . This is in sharp contrast with Beder's model<sup>11</sup> based on the inverse of the  $NN \rightarrow NN\pi$  reaction, which predicts a decreasing energy dependence. [See, however, the remarks on Fermi motion in (2) of Sec. IID below.] We might also mention that a resonancelike behavior for  $\sigma_{\pi, \text{abs}}$  likewise fails to reproduce the data.

Finally, for each  $\sigma_{\rho, \text{abs}}$  and the corresponding  $\sigma_{\pi, \text{abs}}(T)$ , the  $\pi^+/\pi^-$  ratio of total cross sections can be calculated. Comparing with the experimental value<sup>1</sup> of 1.95 for Pb, we find the case of  $\sigma_{\rho, \text{abs}} = 30$  mb works best. This number is close to the limit given in Eq. (16).

The results reported in Sec. IV follow this procedure for fitting  $\sigma_{\rho, \text{abs}}$  and  $\sigma_{\pi, \text{abs}}(T)$ . We have also looked at other kinds of fitting procedures, but found none as good as the one discussed above. The troublesome point is usually trying to get the  $\pi^+/\pi^-$  ratio correct.

The only other input parameters needed for our calculation are the nuclear radii. We use the equivalent uniform sphere values from the compilation of Collard *et al.*,<sup>13</sup> with suitable interpolations and extrapolations where necessary.

#### D. Caveats

As is clear, the fundamental approximation underlying this paper is the use of a semiclassical picture. In addition, however, we have made a number of other approximations for simplicity. We discuss those we are aware of in this section.

(1) Margolis<sup>2</sup> and Glauber<sup>6</sup> have pointed out the importance of using a realistic, diffuse-edge nuclear density. In some scattering and production calculations, a Woods-Saxon distribution gives about twice the cross section obtained from a uniform sphere. We note that introducing a nonuniform density in our model would require that we integrate Eqs. (5) numerically.

(2) Beder<sup>3</sup> has discussed two related Fermi motion corrections which should be folded into the measured  $pp$  production data used in Eqs. (11) and (14). Allowing for Fermi motion will give moderate alterations of the phase-space factors and will give a tail to the spectrum above the free cutoff energy. More important for Beder's calculation at 600 MeV than for ours is a reduction in the effective  $pp$  cross sections due to the proximity of the  $N\Delta$  threshold.<sup>3</sup> Simply stated, a proton striking a target nucleon with an appreciable velocity

component in the incident direction cannot make a  $\Delta$  in this case. This reduction, particularly at the larger pion energies, may account for why Beder was able to obtain a fit to the 600-MeV CERN data with a  $\sigma_{\pi, \text{abs}}(T)$  which decreases with  $T$ .

(3) We estimate that Fermi motion and diffuse-edge corrections for our problem are perhaps 20%. To some extent our empirical procedure for fitting  $\sigma_{\rho, \text{abs}}$  and  $\sigma_{\pi, \text{abs}}$  may have obscured their presence.

(4) The treatment of  $\sigma_{\pi, \text{exch}}$  using Eq. (15) is correct only for pion energies near resonance. It would be straightforward to correct the low- and high-energy charge-exchange cross sections, but we have not done so at this time.

(5) Moreover, the pion charge-exchange cross sections are decreased somewhat in nuclear matter by the Pauli exclusion principle.<sup>3</sup>

(6) Again, the empirical fitting procedure tends to mask the errors due to the approximations discussed in (4) and (5).

(7) In Eq. (5) we assumed that  $\sigma_{\pi, \text{abs}}$ , and hence  $\lambda_a$ , is the same for all pion charges. This is obviously not true but in the absence of information is the simplest thing to do. To take  $\lambda_{a,+} \neq \lambda_{a,0} \neq \lambda_{a,-}$  would introduce two new energy-dependent parameters and would complicate the analytical solution of Eq. (5). Note that if we were to solve Eq. (5) numerically, as we would in the case of a nonuniform density, having unequal  $\lambda_a$ 's would present no further problem other than parameter fitting.

(8) In this respect, the isobar model could be taken as a clue to the charge dependence of  $\sigma_{\pi, \text{abs}}$ , taking  $\pi NN \rightarrow NN$  as the model for the absorption.<sup>11</sup> Equation (10) predicts (when  $N, Z \gg 1$ )

$$\lambda_{a,+} : \lambda_{a,0} : \lambda_{a,-} = \frac{5ZN + \frac{1}{2}N^2}{A^2} : 1 : \frac{5ZN + \frac{1}{2}Z^2}{A^2}. \quad (17)$$

For  $N=Z$ , these ratios are 1.375 : 1 : 1.375, while for  $^{208}\text{Pb}$ , they are 1.38 : 1 : 1.28. In going to the larger nucleus, the  $\pi^+$  absorption is essentially unchanged but the  $\pi^-$  absorption decreases. This will affect the  $\pi^+/\pi^-$  ratio somewhat, lowering it still more for heavier nuclei. Beder,<sup>11</sup> using a more empirical  $\pi NN \rightarrow NN$  amplitude, finds an even more pronounced effect here.

(9) We have not taken into account the possibility of the incident proton undergoing charge-exchange scattering into a neutron. There would be no difficulty in including this effect which should provide yet another way in which the  $\pi^+/\pi^-$  ratio is lowered.

(10) The lack of multiple scattering in our model (straight-line paths in and out) is perhaps most serious in trying to find agreement with the de-

TABLE I. Results for total  $\pi^\pm$  production cross sections, in mb, compared with experimental values taken from Ref. 1.

Nucleus	R (fm)	$\sigma(\pi^+)$		$\sigma(\pi^-)$		$\sigma(\pi^+)/\sigma(\pi^-)$	
		calc	exp	calc	exp	calc	exp
$^9\text{Be}$	3.12	28.8	27.3 $\pm$ 1.4	5.99	6.49 $\pm$ 0.37	4.8	4.3
$^{12}\text{C}$	3.205	36.1	35.0 $\pm$ 1.8	6.54	6.64 $\pm$ 0.41	5.4	5.3
$^{27}\text{Al}$	3.78	50.9	53.1 $\pm$ 2.9	12.5	13.2 $\pm$ 0.9	4.1	4.0
$^{48}\text{Ti}$	4.69	74.0	67.0 $\pm$ 3.6	21.6	21.2 $\pm$ 1.6	3.4	3.2
$^{63}\text{Cu}$	4.97	82.0	77.3 $\pm$ 4.3	25.4	25.2 $\pm$ 2.0	3.2	3.1
$^{108}\text{Ag}$	5.72	97.3	91.6 $\pm$ 5.1	37.5	35.0 $\pm$ 3.0	2.6	2.6
$^{181}\text{Ta}$	7.10	136.2	101.0 $\pm$ 5.6	62.4	51.4 $\pm$ 4.7	2.2	2.0
$^{208}\text{Pb}$	7.11	128.9	104.2 $\pm$ 5.8	64.3	53.7 $\pm$ 4.9	2.0	1.95
$^{232}\text{Th}$	7.37	134.9	107.9 $\pm$ 5.9	70.0	60.4 $\pm$ 5.5	1.9	1.9

tailed angular distributions and energy spectra of  $d^2\sigma/dT d\Omega$ . It is conceivable to go one step further in our model and allow for a secondary scattering at some other point  $\vec{r}'$  in the nucleus. This would introduce more integrations into the calculation with a resulting increase in computing time. Indeed, the ease of calculation is the virtue of our simple model in comparison with a Monte Carlo approach<sup>14</sup> (which has much the same physical basis). Thus there may be no advantage in taking this additional step to this new level of complication.

(11) It is by no means clear that the nuclear radius used here should be the same as that measured in electron scattering.<sup>4</sup>

### III. RESULTS

#### A. Total Cross Sections

Table I gives our results for the  $\pi^\pm$  total production cross sections. The magnitudes of  $\sigma(\pi^+)$  and  $\sigma(\pi^-)$  are in good agreement with the experimental values except for the three largest nuclei, where

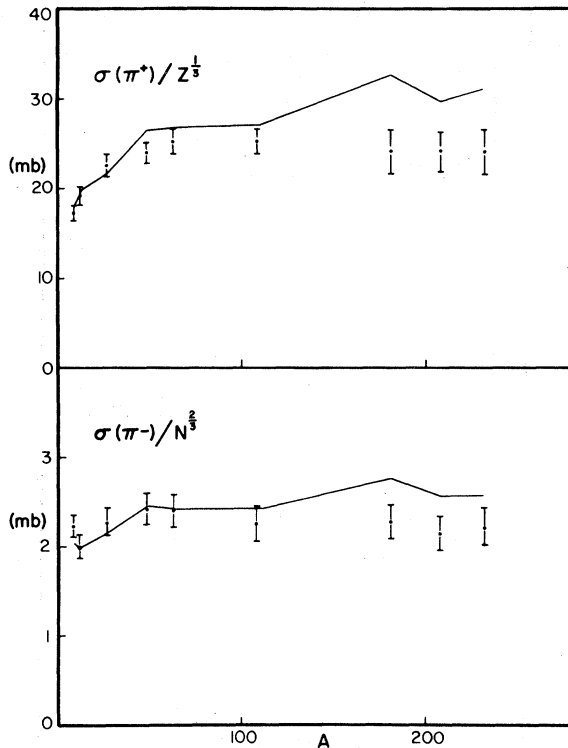


FIG. 3. The scaled total production cross sections  $\sigma(\pi^+)/Z^{1/3}$  and  $\sigma(\pi^-)/N^{2/3}$  versus A. The calculated points are connected by solid lines. Experimental points are taken from Ref. 1.

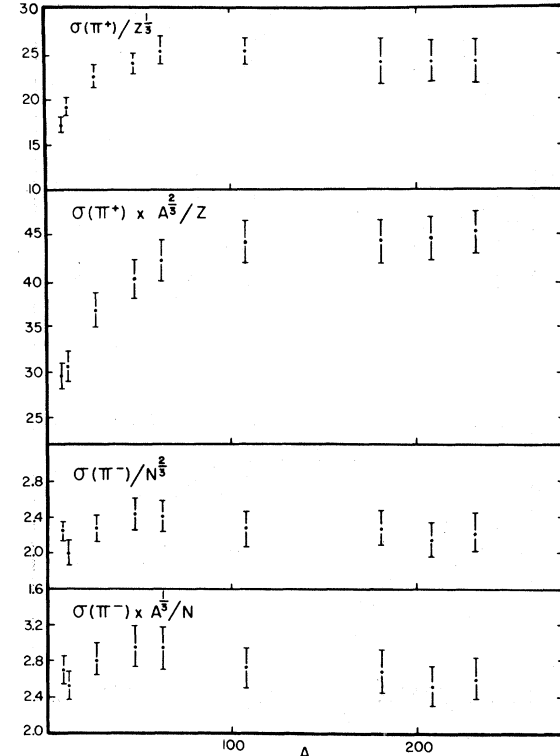


FIG. 4. Comparison of the experimental total production cross sections in mb (taken from Ref. 1) scaled by  $Z^{1/3}$  and  $Z/A^{2/3}$  for  $\pi^+$  and by  $N^{2/3}$  and  $N/A^{1/3}$  for  $\pi^-$ .

both cross sections become large. The predicted  $\pi^+/\pi^-$  ratio is in excellent agreement with experiment for all nuclei.

We emphasize that the agreement shown is obtained by fitting only three parameters:  $\sigma_{\rho,abs}$  and the slope and intercept of the straight-line form for  $\sigma_{\pi,abs}$  (as in Fig. 2). It is difficult to see how the predictions for  $\sigma(\pi^+)$  for large  $A$  could be improved with only  $\sigma_{\rho,abs}$  and  $\sigma_{\pi,abs}(T)$  available as parameters. For, to do so, we must increase the amount of absorption somehow (and have that increase appear mostly at large  $A$ ). But we cannot do this by increasing  $\sigma_{\rho,abs}$ , which is already close to its limiting value as given by Eq. (16). On the other hand, increasing  $\sigma_{\pi,abs}$  will develop difficulties in keeping the  $\pi^+/\pi^-$  ratio small enough to agree with experiment.

Perhaps some of the trouble here is that we are fitting the Pb  $\pi^+/\pi^-$  ratio without any consideration of the contributions to it discussed in our comments (8) and (9) of Sec. IID. If we did not need to make  $\sigma_{\pi,abs}$  so small to get this ratio right, then the larger absorption might lead to a better fit for larger  $A$ .

The calculated cross sections for Ta are some-

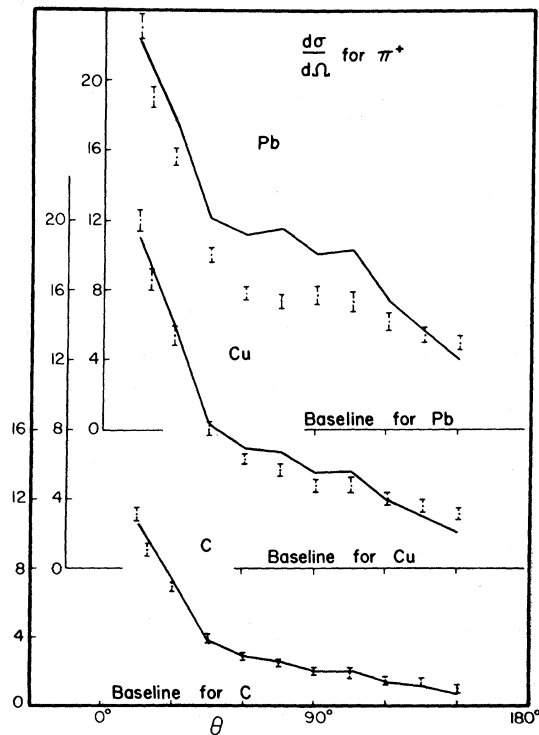


FIG. 5. The angular distributions  $d\sigma/d\Omega$  in mb/sr for  $\pi^+$  production from C, Cu, and Pb. The solid lines connect our calculated values. The roughness in these curves reflects the roughness in the  $pp \rightarrow np \pi^+$  input data. Experimental values are taken from Ref. 1.

what larger than the smooth trend of the other cross sections. This is due to a surprisingly strong dependence of the cross sections on nuclear radius, as is illustrated in Table II for the case of Pb. The dependence of  $\sigma(\pi^+)$  on  $R$  is roughly like  $R^{5/2}$  while that of  $\sigma(\pi^-)$  is more like  $R^2$ . The  $\pi^+/\pi^-$  ratio thus depends on  $R$  as well.

For the case of Ta, a deformed nucleus, the quoted radius<sup>13</sup> is very nearly as big as that for Pb, 7.10 fm vs. 7.11 fm. Thus, with a larger  $Z/N$  ratio, it is not remarkable that the calculated  $\pi^+$  cross section comes out larger than that for Pb. With a smaller radius this would not be so.

The strong dependence on the nuclear radius again suggests that the effects of a diffuse edge for the nuclear density may be important. [See our remark (1) of Sec. IID.] Possibly, a semi-classical model such as this, with appropriate re-

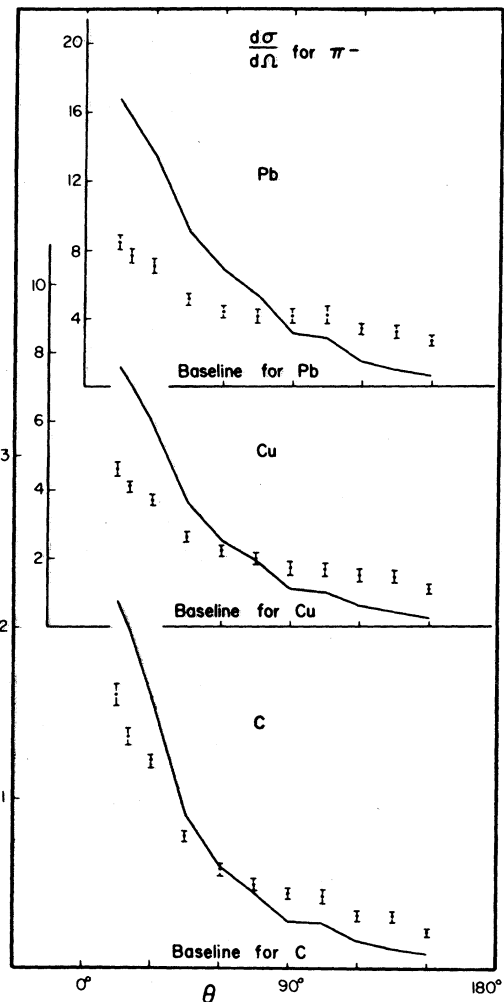


FIG. 6. Same as Fig. 5 but for  $\pi^-$  production. Note, in this case, the different scales for the three nuclei.

TABLE II. Variation of  $\sigma(\pi^\pm)$ , in mb, with the uniform-sphere nuclear radius, for the case of Pb,  $A=208$  fixed.

$R$ (fm)	$\sigma(\pi^+)$	$\sigma(\pi^-)$	$\sigma(\pi^+)/\sigma(\pi^-)$
6.0	83.7	45.8	1.83
7.11	128.9	64.3	2.00
8.00	173.3	79.6	2.18

finements, will allow the extraction of nuclear-surface information from pion-production experiments.

It is evident from Fig. 3 that our calculated total cross sections do not reproduce the experimentally observed near constancy<sup>1</sup> of  $\sigma(\pi^+)/Z^{1/3}$  and  $\sigma(\pi^-)/N^{2/3}$ , mainly because of the too large heavy-nucleus results. Nor have we been successful in constructing a geometrical picture that gives *exactly* these power-law behaviors.

One can estimate that  $\Delta$  production becomes geometric somewhere in the region  $A=20$  to 50. Empirically, the power-law behaviors begin near <sup>27</sup>Al. Thus the initial pion production goes as the area of the disk in which  $\Delta$ 's are made, i.e., proportional to  $A^{2/3}$ .

For the  $\pi^+$  case, the subsequent absorption means that only those  $\pi^+$ 's produced near the rim of this disk will emerge. Thus only a thin ring

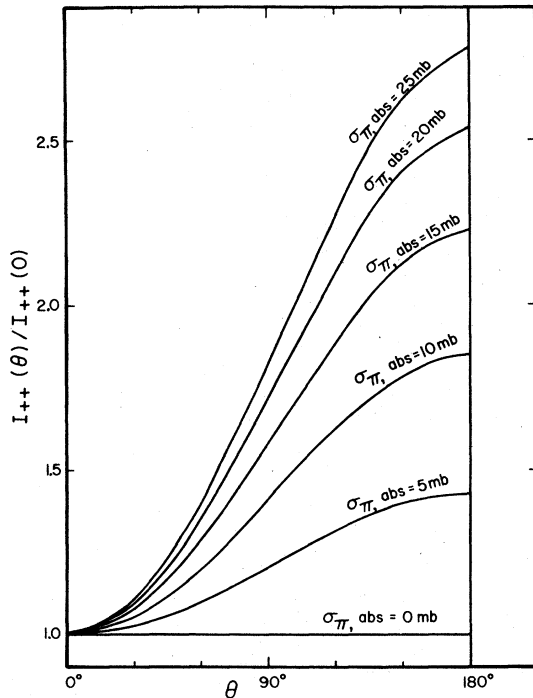


FIG. 7. The angular dependence of  $I_{++}(\theta)/I_{++}(0)$  for the case of  $\pi^+$  production from Pb, with no charge-exchange mixing ( $\sigma_{\pi, \text{exch}} = 0$ ) and a Saxon-Woods nuclear density ( $r_0 = 6.35$ ,  $a = 0.525$  fm). We have taken  $\sigma_{p, \text{abs}} = 30$  mb, together with various constant values of  $\sigma_{\pi, \text{abs}}$ .

contributes significantly to the  $\pi^+$  production, which is an  $A^{1/3}$  dependence. But it is mostly the *protons* in the ring which produce  $\pi^+$ 's, which brings in a factor of  $Z/A$ .<sup>15</sup> Thus we expect  $\sigma(\pi^+)$  to be proportional to  $Z/A^{2/3}$ , which is like  $Z^{1/3}$  to the extent that  $A$  is proportional to  $Z$ .

For the  $\pi^-$  case, the subsequent absorption of the  $\pi^-$ 's is more or less balanced by the charge exchange of  $\pi^0$  into  $\pi^-$ . Thus we expect the  $A^{2/3}$  dependence to be preserved. Since the  $\pi^-$ 's and  $\pi^0$ 's are mainly produced from the neutrons in the disk, we also have a factor of  $N/A$ .<sup>15</sup> Thus  $\sigma(\pi^-)$  should be proportional to  $N/A^{1/3}$ , which to some extent resembles  $N^{2/3}$ .

Figure 4 compares the experimental  $\pi^+$  and  $\pi^-$  production cross sections, as scaled by the various power-law dependences. The differences between the  $Z^{1/3}$  and  $N^{2/3}$  behaviors and the  $Z/A^{2/3}$  and  $N/A^{1/3}$  behaviors, respectively, are small, with the data perhaps slightly favoring the former set.

Note that the arguments presented here for power-law behaviors are not in conflict with a strong  $R$  dependence. The case illustrated in Table II involved a varying nuclear density since  $A$  was held

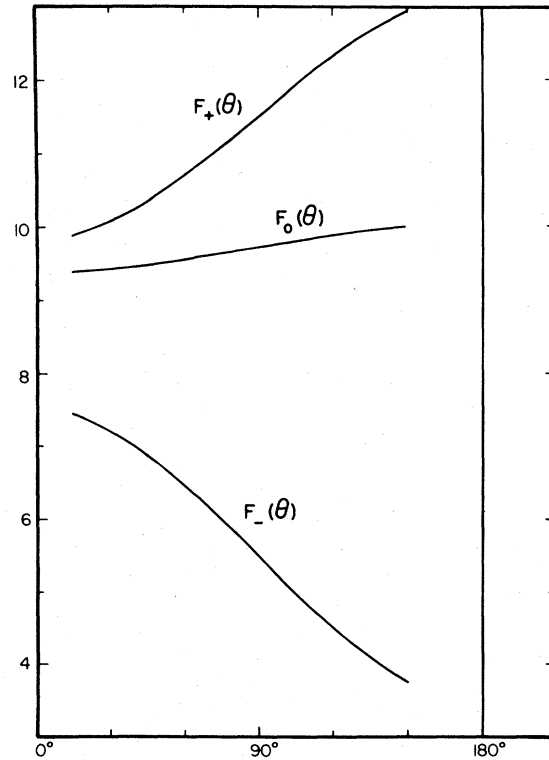


FIG. 8. The angular dependence of  $F_i(T, \theta) = A \sum_j I_{ij}(T, \theta) n_j$  [see Eq. (11)], for the case of Pb at  $T = 105$  MeV with a uniform sphere density ( $R = 7.11$  fm). We have taken  $\sigma_{p, \text{abs}} = 30$  mb,  $\sigma_{\pi, \text{exch}}$  as given by Eq. (15), and the fitted  $\sigma_{\pi, \text{abs}}(T)$  as shown in Fig. 2.

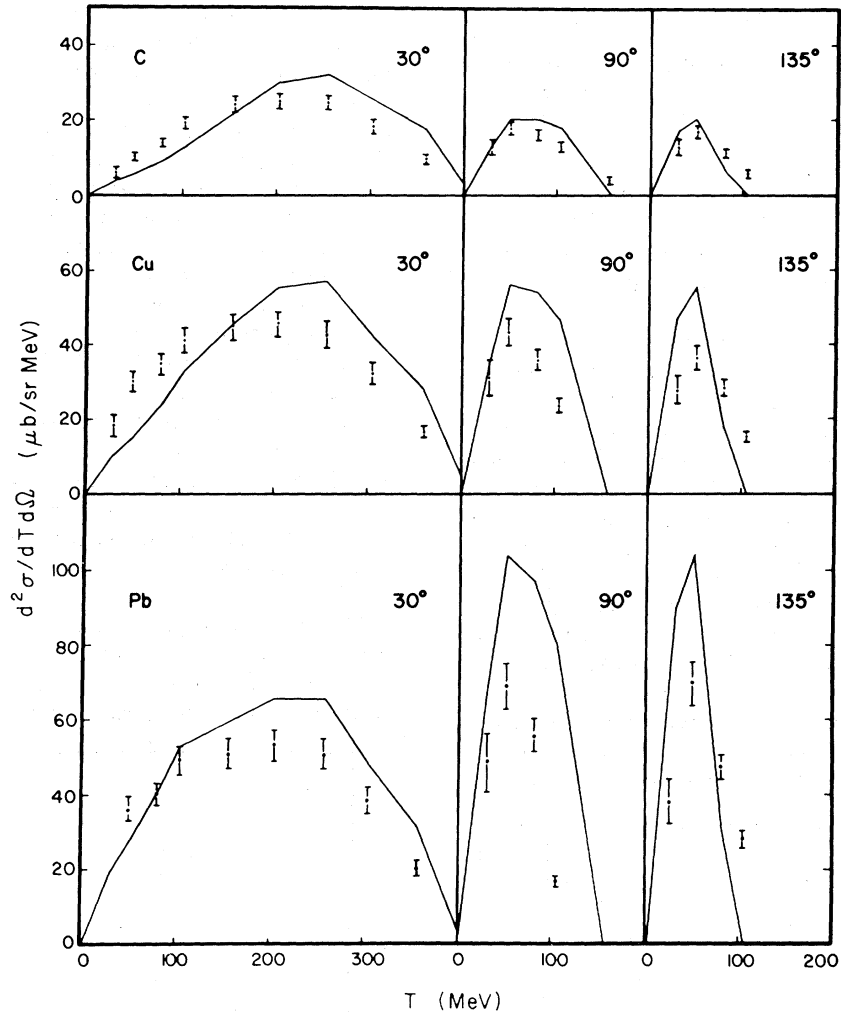


FIG. 9. The  $\pi^+$  spectra  $d^2\sigma/dTd\Omega$  in  $\mu\text{b}/\text{sr MeV}$  for C, Cu, and Pb at  $\theta = 30^\circ, 90^\circ,$  and  $135^\circ$ . The calculated points are connected by solid lines. Experimental points are taken from Ref. 1.

fixed while  $R$  was changed. In the arguments for power-law behaviors we tacitly assumed that  $\rho$  was constant.

#### B. Angular Distributions

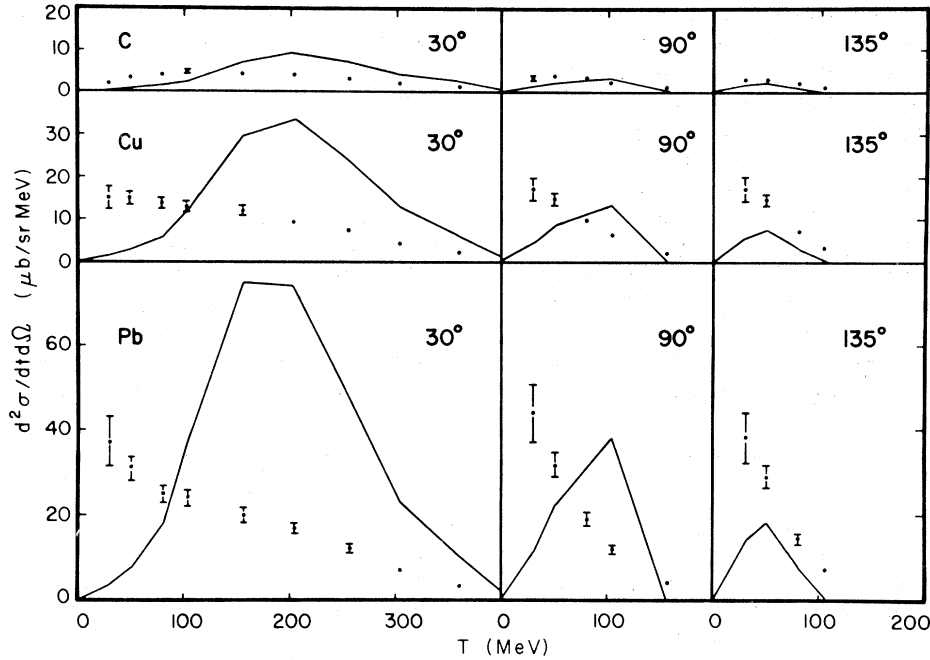
Figure 5 shows some of our results for  $d\sigma(\pi^+)/d\Omega$  obtained by integrating Eq. (11) numerically over  $T$ . The results for C and Cu agree remarkably well with experiment. The calculated cross sections for Pb in the  $45^\circ$  to  $105^\circ$  region are too large, leading to the too large total cross section listed in Table I. [Recall that the  $15^\circ$  Pb cross section is a fitted point in our procedure for obtaining  $\sigma_{p, \text{abs}}$  and  $\sigma_{\pi, \text{abs}}$ .]

The calculated  $\pi^-$  angular distributions are shown in Fig. 6. Again the agreement with experiment is better for the lighter nuclei. It is easy to find a reason why the  $\pi^-$  cross sections here are

systematically too large at small  $\theta$  and too small at large  $\theta$ . The  $\pi^-$ 's are mostly produced in multiple collisions and we have not taken into account any angular dependence for these. The more realistic (and more complicated) treatment mentioned in (10) of Sec. IID would presumably reduce for forward peak, thereby enhancing the backward scattering.

The generally good agreement of our angular distributions with the data could not have been obtained using the forward production approximation for the calculation of the pion path length  $d_\pi$ . Since  $d_\pi$  enters via exponentials, it is not surprising that the error introduced by this approximation is big at large angles. Figure 7 shows this for the situation of Margolis and Kölblig,<sup>16</sup> i.e., a nucleus with a diffuse edge and no charge exchange mixing of the outgoing particles. At the backwards angles, the effective number of  $\pi^+$ 's is enhanced as much



FIG. 10. Same as Fig. 9 but for  $\pi^-$ .

as a factor of two or more. Figure 8 shows the analogous situation for our model, i.e., for a nucleus with a sharp edge and charge exchange mixing of the outgoing pions. The effective number of  $\pi^+$ 's increases with angle, as in Fig. 7, due to the lesser path length for absorption. On the other hand, the effective number of  $\pi^0$ 's at large angles is relatively unchanged from that at small angles, and the effective number of  $\pi^-$ 's even decreases. This last can be understood qualitatively by noting that the  $\pi^-$  population is fed by charge exchange in passing through nuclear matter, as mentioned in Sec. III A. The lesser absorption due to a smaller path length is offset by a lesser charge-exchange production.

### C. Doubly-Differential Cross Sections

Coming now to the fine-detailed predictions of our model, we show in Fig. 9 representative results for  $d^2\sigma(\pi^+)/dTd\Omega$ . As before, the agreement with experiment is better for the lighter nuclei.

In the  $30^\circ$  results there is a tendency for the calculated  $\pi^+$  spectrum to be too low for small  $T$  and too high for large  $T$ . This can again be understood qualitatively as a result of the neglect of multiple scattering. Such collisions would tend to degrade the pion energy, causing a shift and a smearing of the peak of the spectrum.

An interesting thing about the  $90^\circ$  and  $135^\circ$  spectra is, as one goes from C to Pb, the sharp-

ening up and increase relative to the  $30^\circ$  curves.

Figure 10 shows the corresponding calculated  $\pi^-$  spectra. Here the agreement with experiment is relatively poor and gets worse as  $A$  increases. Yet the disagreement can be understood with a more extreme version of the qualitative remarks made above regarding multiple scattering and its effect on the spectra. The  $\pi^-$ 's are mostly produced in charge-exchange processes, so that multiple-scattering corrections are even larger here.

## IV. SUMMARY AND DISCUSSION

We have seen that the isobar production model, as treated in our semiclassical calculation, is consistent with the general features of  $\pi^+$  and  $\pi^-$  production from nuclei. Our inclusion of pion charge exchange has made it possible for the first time to calculate  $\pi^-$  production successfully. Also, dropping the forward production approximation in calculating the pion path length has led to much improved large-angle predictions. Thus the importance of both modifications of the semiclassical model has been established.

The general success of this relatively simple calculation encourages us to go on, making some of the corrections discussed in Sec. IID. As has been suggested,<sup>2,4</sup> it may well turn out that, with improved calculations, we can extract some useful information concerning the nuclear surface from pion production experiments.

In conclusion, we wish to emphasize again the

need for a better knowledge of the parameters which enter a calculation such as this. In particular, as noted in Sec. II C, we badly need some information concerning processes in which a pion enters a nucleus and none emerges. Such experiments, we believe, will be essential for a *general* understanding of pion-nucleus interactions. Although we do not know of current proposals for experiments of this type, we hope that such measurements will be made in the near future at the meson factories scheduled to begin operations soon.

*Note added in proof.* We have been informed by D. S. Beder that the calculation described in Ref.

3 does take into account the angular dependence of  $d_\pi$  and also uses an appropriate nonuniform nuclear density. We thank Dr. Beder for correspondence on these (and other) points.

#### ACKNOWLEDGMENTS

We wish to thank Darragh E. Nagle for bringing this problem to our attention, for encouragement, and for many valuable discussions. Leon Heller, William Kaufman, Arthur Kerman, and H. A. Thiessen contributed useful comments. M. M. S. thanks Louis Rosen and members of the LAMPF staff for their hospitality throughout the past year.

---

\*Work supported in part by the National Science Foundation and the U. S. Atomic Energy Commission. Present address: Department of Physics and Astronomy, University of Massachusetts, Amherst, Massachusetts 01002.

†Work supported by the U. S. Atomic Energy Commission.

<sup>1</sup>D. R. F. Cochran, P. N. Dean, P. A. M. Gram, E. A. Knapp, E. R. Martin, D. E. Nagle, R. B. Perkins, W. J. Shlaer, H. A. Thiessen, and E. D. Theriot, this issue, Phys. Rev. D **6**, 3085 (1972).

<sup>2</sup>B. Margolis, Nucl. Phys. **B4**, 433 (1968).

<sup>3</sup>D. S. Beder and P. Bendix, Nucl. Phys. **B24**, 285 (1971).

<sup>4</sup>R. J. Lombard, J. P. Auger, and R. Basile, Phys. Letters **36B**, 480 (1971); W. Hirt, Nucl. Phys. **B9**, 447 (1969).

<sup>5</sup>R. J. Glauber, in *Lectures in Theoretical Physics*, edited by W. E. Brittin *et al.* (Interscience, New York, 1959), Vol. I, p. 315.

<sup>6</sup>R. J. Glauber, in *High Energy Physics and Nuclear Structure*, edited by G. Alexander (North-Holland, The Netherlands, 1967), p. 311.

<sup>7</sup>D. C. Peaslee, Phys. Rev. **94**, 1085 (1954); **95**, 1580 (1954); S. J. Lindenbaum and R. M. Sternheimer, *ibid.*

**105**, 1874 (1957).

<sup>8</sup>In contrast, Margolis (Ref. 2) assumed the  $\Delta$  does not decay until after it leaves the nucleus.

<sup>9</sup>G. Giacomelli, P. Pini, and S. Stagni, CERN Report No. CERN HERA 69-1, 1969 (unpublished).

<sup>10</sup>O. Benary and L. R. Price, LBL Report No. UCRL-20000 NN 1970 (unpublished).

<sup>11</sup>D. S. Beder, Can. J. Phys. **49**, 1211 (1971).

<sup>12</sup>A heavier nucleus for which data were taken, Th, does not have a known nuclear radius.

<sup>13</sup>H. R. Collard, L. R. B. Elton, and R. Hofstadter, in *Landolt-Börnstein: Numerical Data and Functional Relationships; Nuclear Radii*, edited by K.-H. Hellwege (Springer, Berlin, 1967), New Series, Group I, Vol. 2.

<sup>14</sup>See, e.g., Ref. 1 or H. W. Bertini and M. P. Guthrie, Nucl. Phys. **A169**, 670 (1971). An early Monte Carlo calculation by V. M. Mal'tsev and Yu. D. Prokoshkin, Zh. Eksp. Teor. Fiz. **39**, 1625 (1960) [Sov. Phys. JETP **12**, 1134 (1961)], has also emphasized the importance of charge exchange for obtaining the correct  $\pi^+/\pi^-$  ratio.

<sup>15</sup>This point was emphasized to us by A. K. Kerman, private communication.

<sup>16</sup>K. S. Kölbig and B. Margolis, Nucl. Phys. **B6**, 85 (1968).